

Semiparametric curve alignment and shift density estimation for biological data

T. Trigano, U. Isserles and Y. Ritov

Abstract

Assume that we observe a large number of curves, all of them with identical, although unknown, shape, but with a different random shift. The objective is to estimate the individual time shifts and their distribution. Such an objective appears in several biological applications like neuroscience or ECG signal processing, in which the estimation of the distribution of the elapsed time between repetitive pulses with a possibly low signal-noise ratio, and without a knowledge of the pulse shape is of interest. We suggest an M-estimator leading to a three-stage algorithm: we split our data set in blocks, on which the estimation of the shifts is done by minimizing a cost criterion based on a functional of the periodogram; the estimated shifts are then plugged into a standard density estimator. We show that under mild regularity assumptions the density estimate converges weakly to the true shift distribution. The theory is applied both to simulations and to alignment of real ECG signals. The estimator of the shift distribution performs well, even in the case of low signal-to-noise ratio, and is shown to outperform the standard methods for curve alignment.

Index Terms

semiparametric methods, density estimation, shift estimation, ECG data processing, nonlinear inverse problems.

I. INTRODUCTION

We investigate in this paper a specific class of stochastic nonlinear inverse problems. We observe a collection of $M + 1$ curves

$$y_j(t) = s(t - \theta_j) + \sigma \varepsilon_j(t), \quad t \in [0, T], \quad j = 0 \dots M \quad (1)$$

where the $\varepsilon_0, \dots, \varepsilon_M$ are independent standard white noise processes with variance σ and independent of $\theta_0, \dots, \theta_M$.

Similar models appear commonly in practice, for instance in functional data analysis, data mining or neuroscience. In functional data analysis (FDA), a common problem is to align curves obtained in a series of experiments with varying time shifts, before extracting their common features; we refer to [1] and [2] for an in-depth discussion on the problem of curve alignment in FDA applications. In

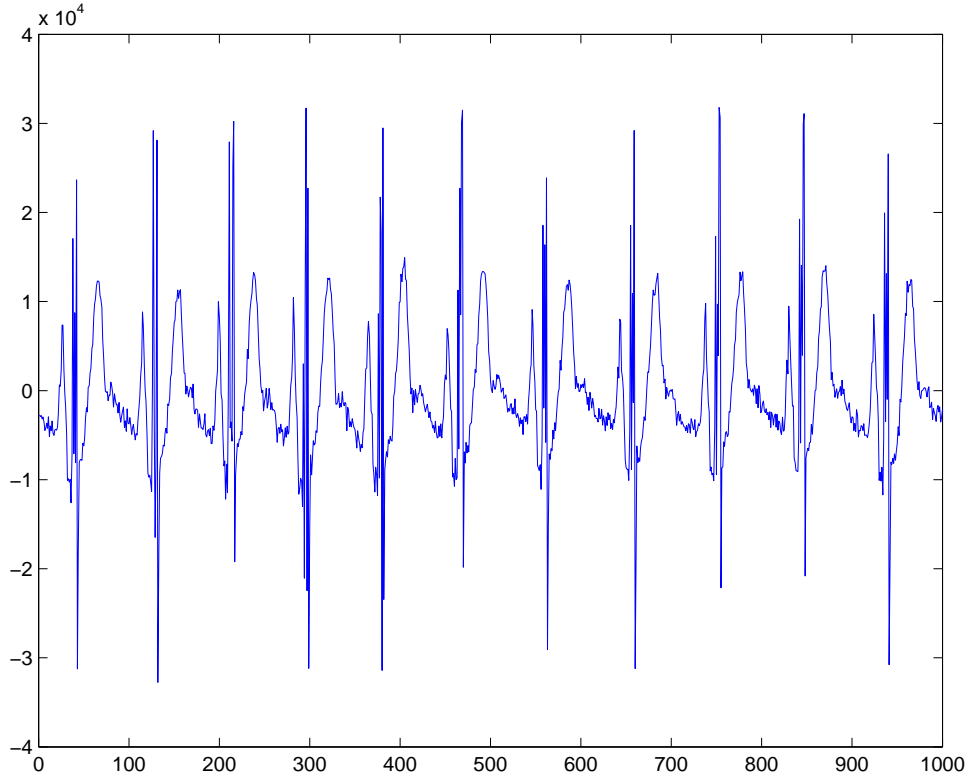


Fig. 1. Example of ECG signal from the MIT-BIH database.

data mining applications, after splitting the data into different homogeneous clusters, observations of a same cluster may differ. Such variations take into account the variability of individual waveforms inside one given group. In the framework described by (1), the knowledge of the translation parameter θ , and more specifically of its distribution, can be used to determine the inner variability of a given cluster of curves. Several papers (see [3], [4], [5], [6], and [7]) focus on this specific model for many different applications in biology or signal processing.

In our main example we analyze ECG signals. In recordings of the heart's electrical activity, at each cycle of contraction and release of the heart muscle, we get a characteristic P-wave, which depicts the depolarization of the atria, followed by a QRS complex stemming from the depolarization of the ventricles and a T-wave corresponding to the repolarization of the heart muscle. We refer to [8, Chapter 12] for an in-depth description of the heart cycle. A typical ECG signal is shown in Figure 1. Different positions of the electrodes, transient conditions of the heart, as well as some malfunctions and several perturbations (baseline wander, powerline interference), can alter the shape of the signal. We aim at situations where the heart electrical activity remains regular enough in the sense that the shape of each cycle remains approximately repetitive, so that after prior segmentation of our recording, the above model still holds. This is the case for heart malfunctions such as sinus tachycardia or supraventricular tachycardia, as mentioned in [8]. This preliminary segmentation can

be done efficiently, for example, by taking segments around the easily identified maxima of the QRS complex, as it can be found in [6], or by means of digital filters as suggested in [9]. It is therefore of interest to estimate the shift parameters θ_j in (1). These estimates can be used afterwards for a more accurate estimation of the heart rate distribution. In normal cases, such estimation can be done accurately by using some common FDA methods (e.g. using only the initial segmentations). However, when the activity of the heart is more irregular, a more precise alignment can be helpful. This happens for example in cases of cardiac arrhythmias, whose identification can be easier if the heart cycles are accurately aligned. Another measurement often used by cardiologists is the mean ECG signal. A problem encountered in that case is that improperly aligned signals can yield an average on which the characteristics of the ECG cycle are lost. The proposed method leads to an estimation of the mean cycle by averaging the segments after an alignment according to an estimated θ_j .

The problem we have to tackle can be seen as an inverse problem. Several authors have investigated nonparametric maximum likelihood estimation for stochastic inverse problems, using variants of the Expectation Maximization (EM) algorithm such as [10]. In our framework, the function s is unknown, thus forbidding the use of such techniques. This is also to relate to semiparametric shift estimation for a finite number of curves and curve alignment problem (see [1]). These problems can be typically encountered in medicine (growth curves) and traffic data. Many methods previously introduced rely on the estimation of s , thus introducing an additional error in the estimation of θ . For example, [6] proposed to estimate the shifts by aligning the maxima of the curves, their position being estimated by the zeros of a kernel estimate of the derivative.

The power spectral density of one given curve remains invariant under shifting, and therefore, it is well fitted for semiparametric methods when s is unknown or the variance of the noise is high. Methods described in [11] or in [12] are based on filtered power spectrum information, and are relevant if the number of curves to reshift is small, which is the case in some applications, such as traffic forecasting. The authors show that their estimator is consistent and asymptotically normal, however, this asymptotic study is done when the number of samples for each curve tends to infinity, the number of curves remaining constant and usually small. On the other hand, it is of interest to investigate the asymptotics for an increasing number of curves, since the duration of the experiment can be more easily controlled than the amount of noise per unit. The asymptotics for an increasing number of curves is presented in this paper.

The paper is organized as follows. Section II describes the assumptions made and the method to derive the estimator of the shift distribution. This method is based on the optimization of a criterion cost, based on the comparison between the power spectra of the average of blocks of curves and the average of the individual power spectrums. Since we consider a large number of curves, we expect that taking the average signal will allow to minimize the cost criterion consistently. We provide in

Section III theoretical results on the efficiency of the method and on the convergence of the density estimate. In Section IV, we present simulations results, which show that the proposed algorithm performs well for density estimation, and study its performances under different conditions. We also applied the methodology to the alignment of ECG curves, and show that the proposed algorithm outperforms the standard FDA methods. Proofs of the discussed results are presented in the appendix.

II. NONPARAMETRIC ESTIMATION OF THE SHIFT DISTRIBUTION

In this section, we present a method for the nonparametric estimation of the shift density. We state the main assumptions that will be used in the rest of the paper, and propose an algorithm which leads to an M-estimator of the shifts. Using these estimators, we obtain a plug-in estimate of the shift probability density function.

A. Assumptions

Assume that we observe $M + 1$ sampled noisy curves on a finite time interval $[0, T]$, each one being shifted randomly by θ ; a typical curve is expressed as

$$\begin{aligned} y_j(t_i) &= s(t_i - \theta_j) + \sigma \varepsilon_j(t_i), \\ t_i &= \frac{(i-1)T}{n}, \quad i = 1 \dots n, \quad j = 0 \dots M. \end{aligned} \tag{2}$$

The processes $\{\varepsilon_j, j = 0 \dots M\}$ are assumed to be standard Gaussian white noises. The variance σ is assumed to be constant. We also assume that we always observe the full noisy curve, which can be formalized by the following assumption:

- (H-1) The distribution of θ and the shape s both have bounded non-trivial support, $[0, T_\theta]$ and $[0, T_s]$, respectively, and $T_\theta + T_s < T$.

As pointed out in [13], under this assumption we can consider s as a periodic function with associated period T . Without any loss of generality, we further assume that $T \triangleq 2\pi$ in order to simplify notations. We also assume:

- (H-2) $s \in L^2([0, T_s])$ and its derivative $s' \in L^\infty$.

Assumption (H-1) implies that we observe a sequence of identical curves with additive noise, so that the spectral information is the same for all curves. Assumption (H-2) guarantees the existence of the Power Spectral Density (PSD) of the studied signal. We denote by f the probability density function of the random variable θ . We also consider the first shift θ_0 as known, and align all the curves with respect to y_0 . Finally, we assume that

- (H-3) The variables $\theta_j, \varepsilon_j(t_i), j = 0, \dots, M, i = 1, \dots, n$ are all independent.

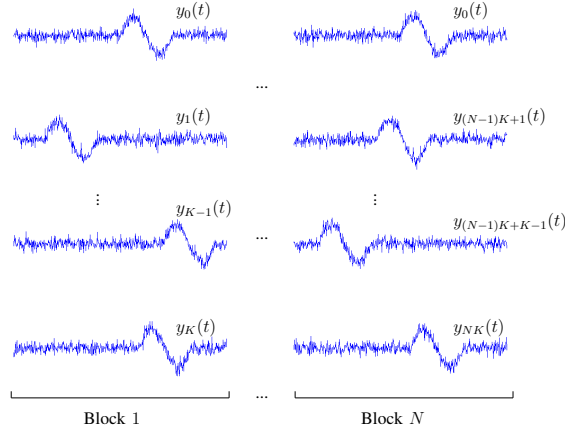


Fig. 2. Split of the curves data set

B. Computation of the estimator

The basic idea of the proposed algorithm is that when the shifts are known and corrected, the signal average has the same shape and PSD as any of the signals. Hence when the shifts are properly corrected, the average of PSD of the individual observed curves is close to the PSD of the average curve. On the other hand, if the shifts are not corrected, then the average signal is a convolution of the original shape with the shift distribution, and hence its PSD is strictly different than the average of the individual PSD's.

Following the method of [14], we propose to plug M estimates of shifts into a kernel estimate. Since we assumed that θ_0 is known, we need to estimate the sequence θ_j , $j = 1 \dots M$. We start by splitting our data set of curves in N blocks of $K + 1$ curves each, as indicated in Figure 2. Observe that the curve y_0 is included in each block, since all the rest of the curves are aligned with it. The motivation to split the data set of curves into blocks is twofold: it reduces the variance of the estimators of the shifts by estimating them jointly, and also provides smooth cost functions for the optimization procedure detailed in this section.

We now describe the criterion function used to estimate θ_m , the vector shift of the m -th block, $m = 1 \dots N$, where for all integer m $\theta_m \triangleq (\theta_{(m-1)K+1}, \dots, \theta_{mK})$. The estimation of θ_m is achieved by minimizing a cost function. We denote by S_y the squared modulus of the Fourier transform of a given continuous curve y , that is for all ω :

$$S_y(\omega) \triangleq \left| \int_0^{2\pi} y(t) e^{-i\omega t} dt \right|^2.$$

This quantity is of interest, since it remains invariant by shifting. For each integer $m = 1 \dots N$, we

define the mean of K curves translated by some correction terms $\alpha_m \triangleq (\alpha_{(m-1)K+1}, \dots, \alpha_{mK})$:

$$\begin{aligned} \bar{y}_m(t; \alpha_m) \\ \triangleq \frac{1}{K + \lambda} \left(\lambda y_0(t) + \sum_{k=(m-1)K+1}^{mK} y_k(t + \alpha_k) \right), \end{aligned} \quad (3)$$

where $\lambda = \lambda(K)$ is a positive number which depends on K , and is introduced in order to give more importance to the reference curve y_0 . For any $m = 1, \dots, N$ we now consider:

$$\frac{1}{M+1} \sum_{k=0}^M S_{y_k} - S_{\bar{y}_m}. \quad (4)$$

The function described in (4) represents the difference between the mean of the PSD (of all observations) and the PSD of the mean curve of the m -th block. Observe that (4) tends to a constant if the curves used in (3) are well aligned, that is when $\alpha_m = \theta_m$. Since the observed curves are sampled, the integral of S_y will be approximated by its Riemann sum, that is

$$\begin{aligned} \hat{S}_y(k) &= \left| \frac{1}{n} \sum_{m=1}^n y(t_m) e^{-2i\pi mk/n} \right|^2, \quad k \in \mathcal{K} \\ \text{where } \mathcal{K} &= \left\{ -\frac{n-1}{2}, -\frac{n-3}{2}, \dots, \frac{n-1}{2} \right\}, \end{aligned}$$

as an estimator of S_y . Let $C_m(\alpha) = \{C_m(k; \alpha) : k \in \mathcal{K}\}$ be defined by

$$C_m(k, \alpha) \triangleq \frac{1}{M+1} \sum_{l=0}^M \hat{S}_{y_l}(k) - \hat{S}_{\bar{y}_m(\cdot; \alpha)}(k). \quad (5)$$

Let $\{\nu_k, k \in \mathcal{K}\}$ be a sequence of nonnegative numbers such that $\nu_{-k} = \nu_k$ and $\sum_k k^2 \nu_k < \infty$ when n tends to infinity. The proposed M-estimator of θ_m , denoted by $\hat{\theta}_m$, is given by

$$\hat{\theta}_m \triangleq \underset{\alpha \in [0; 2\pi]^K}{\text{Arg min}} \|C_m(\alpha)\|_{\nu}^2, \quad (6)$$

where $\|C_m(\alpha)\|_{\nu}^2 = \sum_{k \in \mathcal{K}} \nu_k |C_m(k; \alpha)|^2$.

Remark 2.1: It can be noticed that all blocks of $K+1$ curves have one curve y_0 in common. We chose to build the blocks of curves as described in order to address the problem of identifiability. Without this precaution, replacing the solution of (6) by $\hat{\theta} + c_m$, where c_m is an arbitrary constant, would give the same minimum. Adding the curve y_0 as a reference allows us to estimate $\theta - \theta_0$.

The estimator of the probability density function f , denoted by \hat{f} , is then computed by plugging the estimated values of the shifts in a known density estimator, such as the regular kernel density estimator, that is for all real x in $[0; 2\pi]$:

$$\hat{f}(x) = \frac{1}{(M+1)h} \sum_{m=0}^M \psi \left(\frac{x - \hat{\theta}_m}{h} \right), \quad (7)$$

where ψ is a kernel function integrating to 1 and h the classical tuning parameter of the kernel. In this paper we provide a proof of weak convergence of the empirical distribution function of the individual estimates. More specifically, we shall prove that under some mild conditions

$$\frac{1}{(M+1)} \sum_{m=0}^M g(\hat{\theta}_m) \longrightarrow \mathbb{E}[g(\theta)] ,$$

when both $M \rightarrow \infty$ and $n \rightarrow \infty$, for any bounded continuous function g on $[0, 2\pi]$.

III. THEORETICAL ASPECTS

We provide in this section theoretical results on the convergence of the proposed estimator. Recall that the total number of curves is $M = NK + 1$, where N is the number of blocks and $K + 1$ is the number of curves in each block. The first curve y_0 is a common reference curve which is included in all blocks. We denote by $c_s(k)$ the discrete Fourier transform (DFT) of s taken at point $k \in \mathcal{K}$,

$$c_s(k) \triangleq \frac{1}{n} \sum_{m=1}^n s(t_m) e^{-2i\pi mk/n} ,$$

and by $f_{k,l}$ the discrete Fourier transform of y_l taken at point k :

$$f_{k,l} \triangleq \frac{1}{n} \sum_{m=1}^n y_l(t_m) e^{-2i\pi mk/n} .$$

Let $\theta_l = \bar{\theta}_l + \epsilon_l$ where $|\epsilon_n| < \pi/n$ and $\bar{\theta}_l \in \{t_1, \dots, t_n\}$. Using this notation, relation (2) becomes in the Fourier domain for all $k \in \mathcal{K}$ and $l = 0 \dots M$:

$$\begin{aligned} f_{k,l} &= \frac{1}{n} \sum_{m=1}^n s(t_m - \theta_l) e^{-2i\pi mk/n} \\ &\quad + \frac{\sigma}{\sqrt{n}} (V_{k,l} + iW_{k,l}) \\ &= e^{-ik\bar{\theta}_l} \frac{1}{n} \sum_{m=1}^n s(t_m - \epsilon_l) e^{-2i\pi mk/n} \\ &\quad + \frac{\sigma}{\sqrt{n}} (V_{k,l} + iW_{k,l}) \\ &= e^{-ik\bar{\theta}_l} c_s(k) + O(kn^{-1}) + \frac{\sigma}{\sqrt{n}} (V_{k,l} + iW_{k,l}) , \end{aligned}$$

due to (H-2). The $O(kn^{-1})$ term is a result of the sampling operation and is purely deterministic; since it is assumed that $\sum_k k^2 \nu_k < \infty$, the contribution of this deterministic error to the cost function shall be no more than $O(n^{-1})$, and will further on neglected since it is not going to induce shift estimation errors greater than the length of a single bin (i.e. n^{-1}), while it will be shown that the statistical estimation error is $O_{\mathbb{P}}(n^{-1/2})$. Since we investigate the asymptotic properties of the estimate, especially when both n and K tend to infinity, we hereafter consider this discretization error as negligible and ignore it. By the white noise assumption (H-3), the sequences $\{V_{k,l}, k \in \mathcal{K}\}$ and $\{W_{k,l}, k \in \mathcal{K}\}$ are independent and identically distributed with same standard multivariate normal distribution $\mathcal{N}_n(0, I_n)$.

A. Heuristic argument

Before detailing the complete derivation of the estimate properties, we give in this section a simplified heuristic argument. We assume that both K and n tend to infinity $M \gg K \gg n \rightarrow \infty$, that only one ν_k is different from 0, and that the signal s is an odd function, so that $c_s(k) = ic_k$ is a non-zero imaginary number and there is no reason to align the curves accordingly to y_0 . For simplicity, and without loss of generality, we assume that $\theta_k = 0, k = 0 \dots M$, so that the variables α_l are related to the error made during alignment only. Since M tends to infinity, the mean power spectrum, the first term on the right-hand-side (RHS) of (5), is approximately equal to $c_k^2 + O_{\mathbb{P}}(M^{-1/2})$, so that:

$$\begin{aligned} C_m(k, \alpha) &= c_k^2 + O_{\mathbb{P}}(M^{-1/2}) - \left| \frac{1}{K} \sum_{l=1}^K e^{i\alpha_l k} (\tilde{V}_l + i(c_k + \tilde{W}_l)) \right|^2 \\ &= c_k^2 + O_{\mathbb{P}}(M^{-1/2}) - \left(\frac{1}{K} \sum_{l=1}^K (\tilde{V}_l \cos(\alpha_l k) - (c_k + \tilde{W}_l) \sin(\alpha_l k)) \right)^2 \\ &\quad - \left(\frac{1}{K} \sum_{l=1}^K (\tilde{V}_l \sin(\alpha_l k) + (c_k + \tilde{W}_l) \cos(\alpha_l k)) \right)^2, \end{aligned}$$

where $\tilde{V}_l = \sigma n^{-1/2} V_{k,l}$ and $\tilde{W}_l = \sigma n^{-1/2} W_{k,l}$. Thus we can write:

$$\begin{aligned} C_m(k, \alpha) &= c_k^2 + O_{\mathbb{P}}(M^{-1/2}) - \left(o_{\mathbb{P}}(n^{-1/2}) - \frac{c_k}{K} \sum_{l=1}^K \sin(\alpha_l k) \right)^2 \\ &\quad - \left(o_{\mathbb{P}}(n^{-1/2}) + \frac{c_k}{K} \sum_{l=1}^K \cos(\alpha_l k) \right)^2 \\ &= c_k^2 + O_{\mathbb{P}}(M^{-1/2}) + o_{\mathbb{P}}(n^{-1/2}) - \frac{c_k^2}{K^2} \sum_{1 \leq l, m \leq K} \cos(k(\alpha_l - \alpha_m)) \\ &= O_{\mathbb{P}}(M^{-1/2}) + o_{\mathbb{P}}(n^{-1/2}) + c_k^2 \sum_{1 \leq l, m \leq K} \frac{1 - \cos(k(\alpha_l - \alpha_m))}{K^2} \end{aligned}$$

From the latter equation, it can be shown that a minimum of $|C_m(k, \alpha)|$ can be obtained when all variables α_l are equal. Moreover, there exists two constants C_1 and C_2 such that:

$$\begin{aligned} O_{\mathbb{P}}(M^{-1/2}) + o_{\mathbb{P}}(n^{-1/2}) + C_1 \left(\frac{1}{K^2} \sum_{1 \leq l, m \leq K} (\alpha_l - \alpha_m)^2 \right)^2 \\ \leq \|C_m(\alpha)\|_{\nu}^2 \leq O_{\mathbb{P}}(M^{-1/2}) + o_{\mathbb{P}}(n^{-1/2}) + C_2 \left(\frac{1}{K^2} \sum_{1 \leq l, m \leq K} (\alpha_l - \alpha_m)^2 \right)^2, \end{aligned}$$

thus, when both M and n tend to infinity, we can only attain the minimum of the cost function when all the variables α_m are equal, that is when the curves are well aligned.

B. Computation of the cost function C_m

The cost function C_m associated with block m can be written as follows:

$$\begin{aligned} \|C_m(\boldsymbol{\alpha}_m)\|_{\nu}^2 &= \sum_{k \in \mathcal{K}} \nu_k (A_M(k) - B_m(k, \boldsymbol{\theta}_m))^2 \\ &+ \sum_{k \in \mathcal{K}} \nu_k (B_m(k, \boldsymbol{\theta}_m) - B_m(k, \boldsymbol{\alpha}_m))^2 \\ &+ 2 \sum_{k \in \mathcal{K}} \nu_k (B_m(k, \boldsymbol{\theta}_m) - B_m(k, \boldsymbol{\alpha}_m)) \\ &\quad \times (A_M(k) - B_m(k, \boldsymbol{\theta}_m)), \end{aligned} \quad (8)$$

where $A_M(k)$ and $B_m(k, \boldsymbol{\alpha}_m)$ are the first and second terms of the right hand side (RHS) of (5), both taken at point k . Each term of the latter equation is expanded separately. We get that

$$\begin{aligned} A_M(k) &= |c_s(k)|^2 + \frac{\sigma^2}{(M+1)n} \sum_{l=0}^M (V_{k,l}^2 + W_{k,l}^2) \\ &+ \frac{2\sigma \text{Re}(c_s(k))}{(M+1)\sqrt{n}} \sum_{l=0}^M (V_{k,l} \cos(k\theta_l) - W_{k,l} \sin(k\theta_l)) \\ &- \frac{2\sigma \text{Im}(c_s(k))}{(M+1)\sqrt{n}} \sum_{l=0}^M (V_{k,l} \sin(k\theta_l) + W_{k,l} \cos(k\theta_l)) \end{aligned} \quad (9)$$

Remark 3.1: By Assumption (H-2) and the law of large numbers the last two terms of (9) converge almost surely to 0 as M tends to infinity. Moreover, the sum of the second term has a χ^2 distribution with $2(M+1)$ degrees of freedom. Thus, the term $A_M(k)$ tends to $|c_s(k)|^2 + 4n^{-1}\sigma^2$ as $M \rightarrow \infty$, and therefore to $|c_s(k)|^2$ as both M and n tend to infinity.

Recall that $B_m(k, \boldsymbol{\alpha}_m)$ is the modulus of the squared DFT of the average of the curves in block m , after shift correction. We focus on the expansion of the terms associated with $\|C_1(\boldsymbol{\alpha}_1)\|_{\nu}^2$, since all other cost functions may be expanded in a similar manner up to a change of index. The first curve of each block is the reference curve, which is considered to be invariant and thus has a known associated shift $\alpha_0 = \theta_0 = 0$. We obtain

$$\begin{aligned} B_1(k, \boldsymbol{\alpha}_1) &= \left| \frac{1}{\lambda + K} \left[\lambda(c_s(k) + \frac{\sigma}{\sqrt{n}}(V_{k,0} + iW_{k,0})) \right. \right. \\ &\quad \left. \left. + \sum_{l=1}^K \left(e^{ik(\alpha_l - \theta_l)} c_s(k) + \frac{\sigma}{\sqrt{n}} e^{ik\alpha_l} (V_{k,l} + iW_{k,l}) \right) \right] \right|^2, \end{aligned}$$

thus, if we define λ_m , $m = 0 \dots K$, such that $\lambda_0 \triangleq \lambda$ and $\lambda_m \triangleq 1$ otherwise:

$$\begin{aligned}
B_1(k, \boldsymbol{\alpha}_1) &= \frac{|c_s(k)|^2}{(\lambda + K)^2} \sum_{l,m=0}^K \lambda_l \lambda_m e^{ik(\alpha_l - \theta_l - \alpha_m + \theta_m)} \\
&+ \frac{\sigma^2}{n(\lambda + K)^2} \sum_{l,m=0}^K \lambda_l \lambda_m \{e^{ik(\alpha_l - \alpha_m)} \times \\
&[V_{k,l}V_{k,m} + W_{k,l}W_{k,m} + i(V_{k,l}W_{k,m} - W_{k,l}V_{k,m})]\} \\
&+ \frac{\sigma c_s(k)}{\sqrt{n}(\lambda + K)^2} \sum_{l,m=0}^K \lambda_l \lambda_m e^{i(\alpha_l - \theta_l - \alpha_m)} (V_{k,m} - iW_{k,m}) \\
&+ \frac{\sigma c_s^*(k)}{\sqrt{n}(\lambda + K)^2} \sum_{l,m=0}^K \lambda_l \lambda_m e^{ik(\theta_m + \alpha_l - \alpha_m)} (V_{k,l} + iW_{k,l}) .
\end{aligned} \tag{10}$$

The functional $\|C_1(\boldsymbol{\alpha}_1)\|_{\nu}^2$ can be split into a stochastic part which depends on V and W , and a noise-free part, which neither depends on $\{V_{k,l}, k = -\frac{n-1}{2} \dots \frac{n-1}{2}\}$ nor $\{W_{k,l}, k = -\frac{n-1}{2} \dots \frac{n-1}{2}\}$, and is further on denoted by $D_1(\boldsymbol{\alpha}_1)$. This term is equal to:

$$\begin{aligned}
D_1(\boldsymbol{\alpha}_1) & \\
&= \sum_{k \in \mathcal{K}} \nu_k |c_s(k)|^4 \left| \left| \frac{1}{K + \lambda} \sum_{m=0}^K \lambda_m e^{ik(\alpha_m - \theta_m)} \right|^2 - 1 \right|^2
\end{aligned} \tag{11}$$

Details of the calculations are given in Appendix A. Note that due to (11), D_1 has a unique global minimum which is attained when $\alpha_m = \theta_m$, for all $m = 1 \dots, K$, that is the actual shift value. We show in Proposition 3.1 that $\|C_1(\boldsymbol{\alpha}_1)\|_{\nu}^2 - D_1(\boldsymbol{\alpha}_1)$ is negligible when both n and K tend to infinity, under mild assumptions on λ , so that the proposed cost function behaves asymptotically like $D_1(\boldsymbol{\alpha}_1)$. Due to (8), terms which depend on V and W stem from $A_M(k) - B_1(k, \boldsymbol{\theta}_1)$ and $B_1(k, \boldsymbol{\theta}_1) - B_1(k, \boldsymbol{\alpha}_1)$.

Proposition 3.1: Assume that $K \rightarrow \infty$, $n \rightarrow \infty$, $\lambda \rightarrow \infty$, and $\lambda/K \rightarrow 0$. Denote the noise part associated with $B_1(k, \boldsymbol{\theta}_1) - B_1(k, \boldsymbol{\alpha}_1)$ by $R(k)$. Then:

$$\begin{aligned}
\sum_{k \in \mathcal{K}} \nu_k (A_m(k) - B_1(k, \boldsymbol{\theta}_1))^2 &= O_{\mathbb{P}} \left(\frac{1}{nK} \right) \\
\sum_{k \in \mathcal{K}} \nu_k R(k)^2 &= O_{\mathbb{P}} \left(\frac{1}{n^2} \right) + O_{\mathbb{P}} \left(\frac{1}{nK} \right) \\
\sum_{k \in \mathcal{K}} \nu_k (A_m(k) - B_1(k, \boldsymbol{\theta}_1)) (B_1(k, \boldsymbol{\alpha}_1) - B_1(k, \boldsymbol{\theta}_1)) &= O_{\mathbb{P}} \left(\frac{1}{\sqrt{nK}} \right) .
\end{aligned} \tag{12}$$

Proof: See Appendix B. ■

Since $\hat{\theta}_1$ is the minimizer of C_1 and $D_1(\theta_1) = 0$, we get by means of Proposition 3.1 that

$$\begin{aligned}
 D_1(\hat{\theta}_1) &= C_1(\hat{\theta}_1) + (D_1(\hat{\theta}_1) - C_1(\hat{\theta}_1)) \\
 &\leq C_1(\theta_1) + (D_1(\hat{\theta}_1) - C_1(\hat{\theta}_1)) \\
 &= D_1(\theta_1) + (D_1(\hat{\theta}_1) - C_1(\hat{\theta}_1)) \\
 &\quad - (D_1(\theta_1) - C_1(\theta_1)) \\
 &= (D_1(\hat{\theta}_1) - C_1(\hat{\theta}_1)) \\
 &\quad - (D_1(\theta_1) - C_1(\theta_1)) \\
 &= O_{\mathbb{P}}\left(\frac{1}{n^2}\right) + O_{\mathbb{P}}\left(\frac{1}{\sqrt{nK}}\right),
 \end{aligned}$$

thus showing that $D_1(\hat{\theta}_1)$ is close to zero as both n and K tend to infinity. The following result gives information on the number of curves well aligned in a given block, and holds for each term in the sum of Equation (11).

Proposition 3.2: Let $\eta \rightarrow 0$ as $n, K \rightarrow \infty$, and let δ be a real positive number. Assume that for some $k \in \mathcal{K}$:

$$\left| \frac{1}{(K + \lambda)} \sum_{m=0}^K \lambda_l e^{ik(\theta_m - \alpha_m)} \right| > 1 - \eta,$$

then there exists two positive constants γ_0 and K_0 , such that for $K \geq K_0$, there is a constant c such that the number of curves whose alignment error $\alpha_m - \theta_m - c$ is bigger than η^δ , is bounded by $\gamma_0(K + \lambda)\eta^{1-2\delta}$. Moreover,

$$\sum_{m=1}^K (\theta_m - \alpha_m - c)^2 \leq \frac{(K + \lambda)\eta}{\gamma_0 k^2}. \quad (13)$$

Proof: See Appendix C. ■

Proposition 3.2 has the following motivation: when the number of curves in each block is large enough, the noise contribution to the criterion will be small, and $\hat{\theta}_1$ will be such that the condition of the proposition holds. Hence, we can conclude that most curves will tend to align. However, they may not align with the reference curve y_0 . Consequently, the weighting factor λ is introduced in order to “force” all the curves in a block to align with respect to y_0 , as stated in the following proposition:

Proposition 3.3: Assume that λ is an integer, and that $\eta^{1-2\delta} \leq \lambda/(\gamma(K + \lambda))$. Then, under the assumption of Proposition 3.2, we get that $|c| < \eta^\delta$

Proof: See Appendix D. ■

In other words, when λ is chosen such that $\lambda \rightarrow \infty$ and $\lambda/K \rightarrow 0$ as $K \rightarrow \infty$, the estimate would be close to the actual shifts.

Theorem 3.1: Under Assumptions (H-1)–(H-3), if $K \rightarrow \infty$, $n \rightarrow \infty$, $\lambda = \lambda(K) \rightarrow \infty$, $\lambda/K \rightarrow 0$, and n/K is bounded, then for all $\delta \in (0, 1/2)$, there exists $\gamma > 0$, such that with probability converging to 1

$$\frac{1}{K + \lambda} \sum_{m=1}^K \mathbf{1}(|\hat{\theta}_m - \theta_m| > 2n^{-\delta}) \leq \gamma n^{-(1-2\delta)}.$$

$$\exists c < n^{-\delta} : \quad \frac{1}{K + \lambda} \sum_{m=1}^K (\hat{\theta}_m - \theta_m - c)^2 \leq \gamma n^{-1}.$$

Proof of this theorem can be easily deduced from Proposition 3.2 and 3.3 by choosing $\eta = n^{-1}$ and writing $\mathbf{1}(|\hat{\theta}_m - \theta_m| > 2n^{-\delta}) = \mathbf{1}(|\hat{\theta}_m - \theta_m - c + c| > 2n^{-\delta})$ in the latter equation.

C. Weak convergence of the density estimator

Due to the previous results, it is now possible to give a theoretical result about the plug-in estimate of the distribution of θ . As suggested in (7), an estimate of the probability density function f can be obtained by plugging the approximated values of the shifts into a known density estimate. We provide here a result on the weak convergence of the empirical estimator.

Theorem 3.2: Let g be a continuous function with a bounded derivative. Under the assumptions of Theorem 3.1, we get almost surely when $M \rightarrow \infty, n \rightarrow \infty$ that

$$\frac{1}{M+1} \sum_{k=0}^M g(\hat{\theta}_k) \rightarrow \mathbb{E}[g(\theta)]. \quad (14)$$

Proof of theorem 3.2 can be sketched as follows: due to the Law of Large Numbers, it is equivalent to show that:

$$\frac{1}{M+1} \sum_{k=0}^M (g(\hat{\theta}_k) - g(\theta_k))$$

converges almost surely to 0. Since g has a bounded derivative, we can write that the absolute value of the latter term is bounded by

$$\frac{\sup_x |g'(x)|}{M+1} \sum_{k=0}^M |\hat{\theta}_k - \theta_k|.$$

Consequently, due to Theorem 3.1, there exists a constant C such that:

$$\frac{1}{M+1} \sum_{k=0}^M (g(\hat{\theta}_k) - g(\theta_k)) \leq C \left(\frac{1}{Nn^\delta} + \frac{\gamma}{Nn^{1-2\delta}} \right),$$

thus showing convergence almost surely.

Remark 3.2: If n remains bounded as $K \rightarrow \infty$, then the parameters θ_m cannot be estimated, and the observed distribution of $\{\hat{\theta}_m\}$ would be a convolution of the distribution of $\{\theta_m\}$ with the estimation error. If n is large enough, the latter distribution is approximately normal with variance which is $O_{\mathbb{P}}(\sigma^2/n)$.

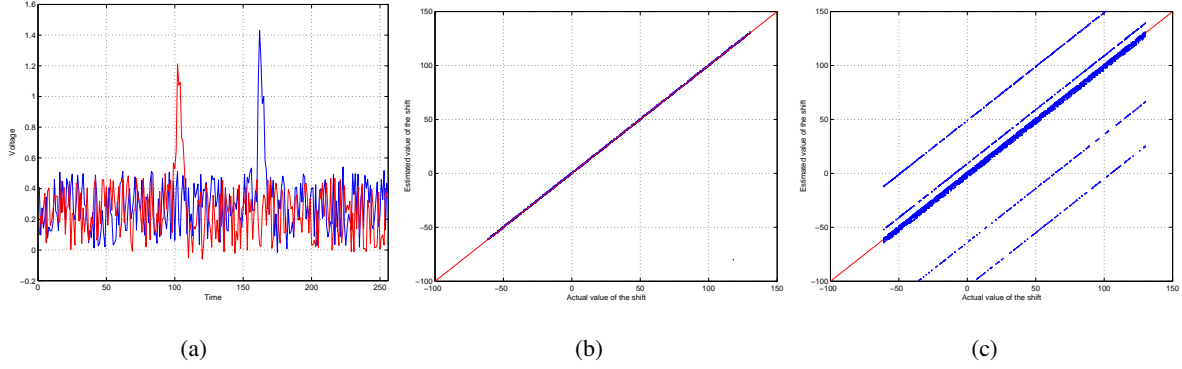


Fig. 3. Results for $K=200$ and $\sigma^2 = 0.1$; (a) two curves before alignment. (b) comparison between estimated against actual values (blue dots) of the shifts for $\lambda = 50$: good estimates must be close of the identity line (red curve). (c) comparison between estimated and actual values of the shifts for $\lambda = 10$.

IV. APPLICATIONS

We present in this section results based both on simulations for the neuroscience framework and on real ECG data. In the latter case, we compare our method to the one described in [1] which is often used by practitioners, that is a measure of fit based on the squared distance between the average pulse and the shifted pulses leading to a standard Least Square Estimate of the shifts. A method for choosing automatically the best parameter K has been proposed in the related conference paper [15].

A. Simulations results

Using simulations we can study the influence of the parameters K and λ empirically by providing the Mean Integrated Squared Error (MISE) for different values of K and σ^2 . We use a fixed number of blocks $N = 20$. The weighting parameter is chosen as $\lambda = [K^\beta]$, where $0 < \beta < 1$. Choosing β close to 1 enables us to align the curves of a given block with respect to the reference curve.

1) *Experimental protocol*: Simulated data are created according to the discrete model (1), and we compute the estimators for different values of the parameters K , λ and σ^2 . For each curve, we sample 512 points equally spaced on the interval $[0; 2\pi]$. We make the experiment with s computed according to the standard Hodgkin-Huxley model for a neural response. The shifts are drawn from a uniform distribution $\mathcal{U}(120\pi/256, 325\pi/256)$, and $\theta_0 = \pi$.

2) *Results*: We present in Figure 3 results obtained using the alignment procedure, in the case of high noise level ($\sigma^2 = 0.1$). We also compare our estimations with those obtained with an existing method, namely curve alignment according to the comparison between each curve to the mean curve [1]. Results using landmark alignment are displayed in Figure 5. We observe that the efficiency of this approach is less than our estimate achieves with $\lambda = 50$, Figure 3-(b), but is better than the estimate with $\lambda = 10$, Figure 3-(c). An example of density estimation is displayed in Figure 4,

σ^2	K=10	K=20	K=30	K=50	K=100
0	0.0305	0.0228	0.0198	0.0153	0.0106
	0.0306	0.0234	0.0199	0.0156	0.0109
10^{-4}	0.0312	0.0218	0.0183	0.0156	0.0121
	0.0325	0.0232	0.0212	0.0183	0.0158
10^{-2}	0.0296	0.0218	0.0172	0.0143	0.0120
	0.0306	0.0232	0.0192	0.0172	0.0143
1	0.0326	0.0274	0.0248	0.0255	0.0288
	0.0547	0.0806	0.0514	0.0553	0.0741

TABLE I
THE MISE OF THE TWO DENSITY ESTIMATES.

using a uniform kernel. We retrieve the uniform distribution of θ . Table I shows the estimated MISE for different values of K and σ^2 , with $\lambda = [K^{0.9}]$ and $N = 100$ blocks. The first given number is the value for our estimate, while the second is for the estimator of [1]. Note the dominance of the proposed estimator in all cases, in particular for the more noisy situations.

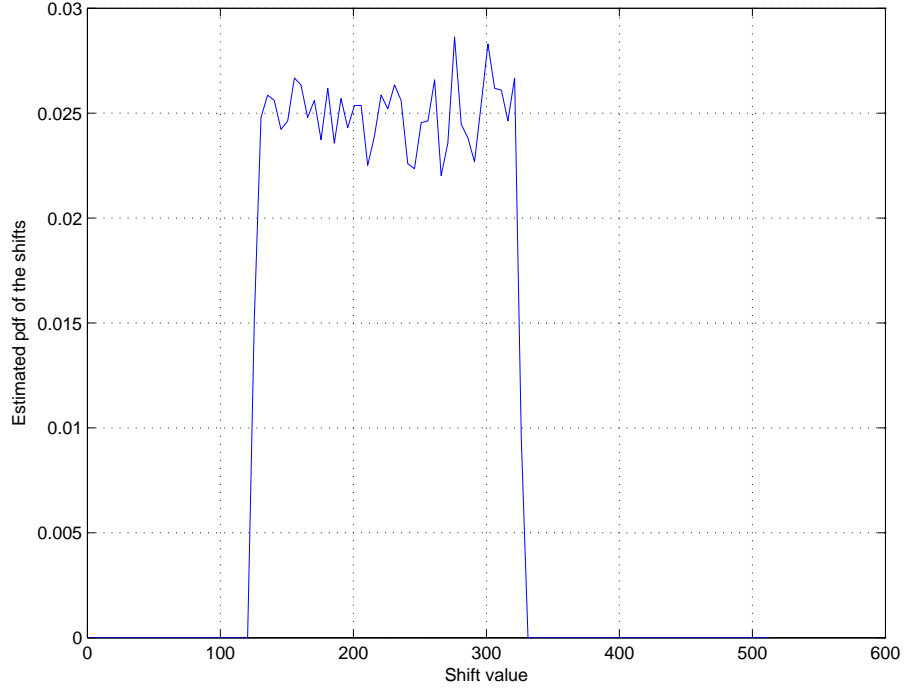


Fig. 4. Probability density estimation for $N = 20$, $K = 200$ and $\sigma^2 = 0.1$.

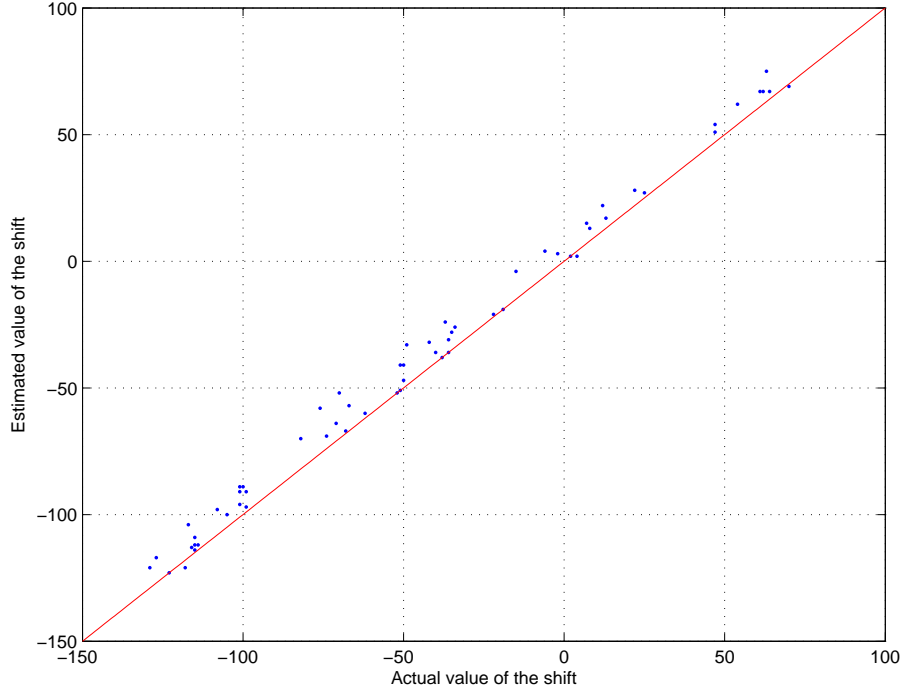


Fig. 5. Shift estimation using Least Square Estimate (see [1]) for one block.

B. Results on real data

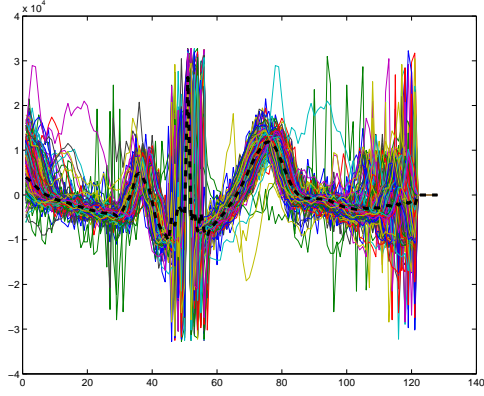
We now compared the estimated average aligned signal of the two methods applied to the heart cycles presented in Figure 1. The data was obtained from the Hadassah Ein-Karem hospital.

1) *Experimental protocol:* In order to obtain a series of heart cycles, we first make a preliminary segmentation using the method of [6], namely alignment according to the local maxima of the heart cycle. We then apply our method, and compare it to the alignment obtained by comparing the mean curve to a shifted curve one at a time. We took in this example $K = 30$ and $\lambda = K^{0.75}$.

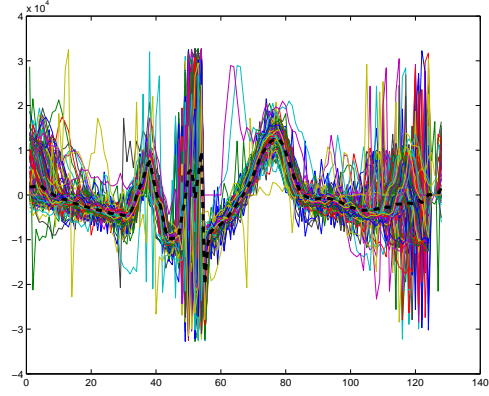
2) *Results:* The results are presented in Figure 6. Comparison of Figures 6(c) and 6(d) shows that the proposed method outperforms the standard method. Moreover, when computing the average of the reshifted heart cycle, we observe that our method allows to separate more efficiently the different parts of the heart cycle; indeed, the separation between the P-wave, the QRS-complex and the T-wave are much more visible, as it can be seen by comparing the average signals obtained in Figure 6(a) and Figure 6(b).

C. Influence of ECG perturbations on the proposed algorithm

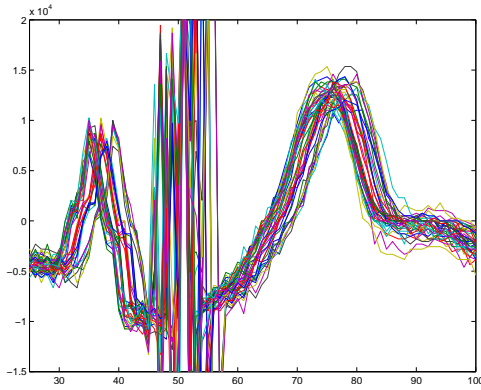
As we saw, the model fits reasonably well the data we have at hand, and in fact perform better than the competing algorithm. The ideal model may not fit other data sets in which the shape of the heart pulse changes, or additional perturbations occur. Although no estimation procedure can operate



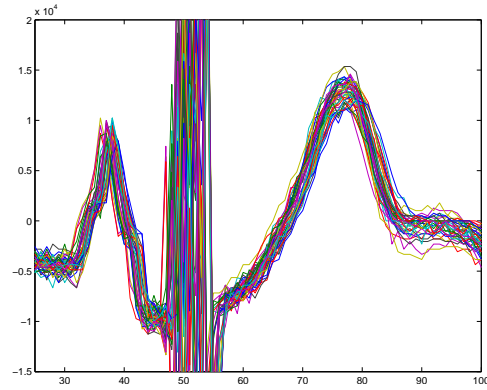
(a) Aligned heart cycles and average signal (black dotted curve) using the standard method



(b) Aligned heart cycles and average signal (black dotted curve) using the proposed method



(c) Aligned heart cycles using the standard method, zoom for the first 30 curves



(d) Aligned heart cycles using the proposed method, zoom for the first 30 curves

Fig. 6. Comparison between the state-of-the-art and the proposed method for the alignment of heart cycles (arbitrary units). A semiparametric approach appears more appealing to align cycles according to their starting point, and allows to separate more efficiently to P-wave, the QRS complex and the T-wave.

under any possible distortion of the data, we now show that our procedure is quite robust against the main type of potential distortions. The main type of perturbations related to the processing of ECG data are of four kinds (cf. [16]):

- the baseline wandering effect, which can be modeled by the addition of a very low-frequency curve.
- 50 or 60 Hz power-line interference, corresponding to the addition of an amplitude and frequency varying sinusoid.
- Electromyogram (EMG), which is an electric signal caused by the muscle motion during effort test.
- Motion artifact, which comes from the variation of electrode-skin contact impedance produced by electrode movement during effort test.

To keep the discussion within the scope of the paper, we chose to focus on two perturbations, namely the baseline wander effect and the power-line interference effect. We present in Figure 7 the effect of baseline wander on the proposed algorithm. This effect was simulated by the addition of a low-frequency sine to the ECG measurements. We took here $N = 100$, $K = 100$, $\lambda = K^{0.9}$.

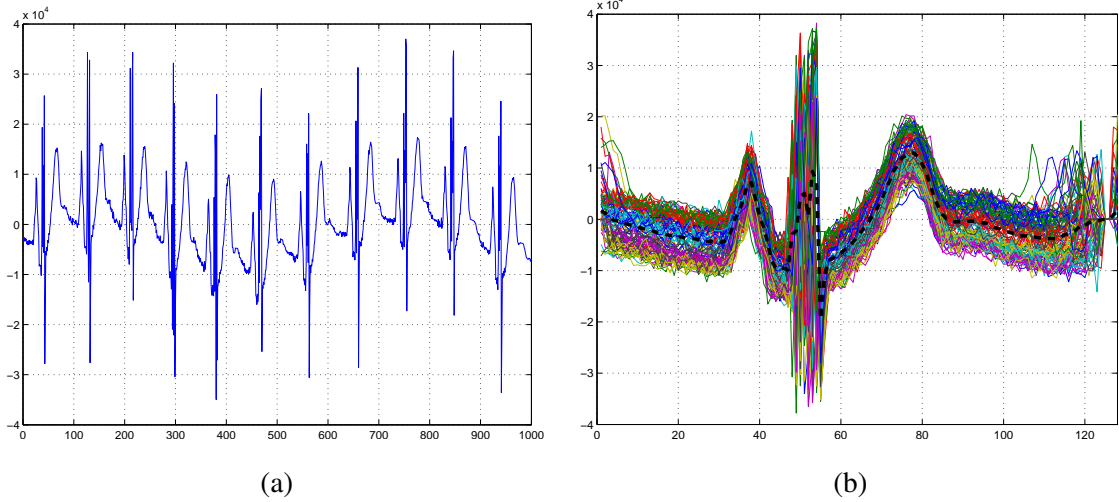


Fig. 7. Effect of the baseline wander phenomenon over the proposed curve alignment method: distorted signal (a), and aligned pulses with the average ECG pulse obtained for one block (b)

We observe that the proposed curve alignment algorithm is robust regarding this kind of perturbations, since we observe well-aligning curves and very little change on the average pulse shape compared to the one obtained without this perturbation. This can be interpreted as follows: since the baseline is in this situation a zero-mean process, the averaging which is done while computing the cost function naturally tends to cancel the baseline. However, we remark that the baseline wander phenomenon can cripple the preliminary segmentation, if the amplitude of the baseline is too high. This problem can be easily circumvented by means of a baseline reduction prefiltering, such as proposed in [16], [17], [18].

We now consider the problem of powerline interference. In order to artificially simulate the original signal with a simulation of the powerline interference, we used the model described in [19], that is, we add to the ECG signal the following discrete perturbation:

$$y[n] = (A_0 + \xi_A[n]) \sin \left(\frac{2\pi(f_0 + \xi_f[n])}{f_s} n \right),$$

where A_0 is the average amplitude of the interference, f_0 its frequency, f_s the sampling frequency of the signal and $\xi_A[n], \xi_f[n]$ are white Gaussian processes used to illustrate possible changes of the amplitude and frequency of the interference. The results of the curve alignment procedure are presented in Figure 8, for a similar choice of N , K and λ .

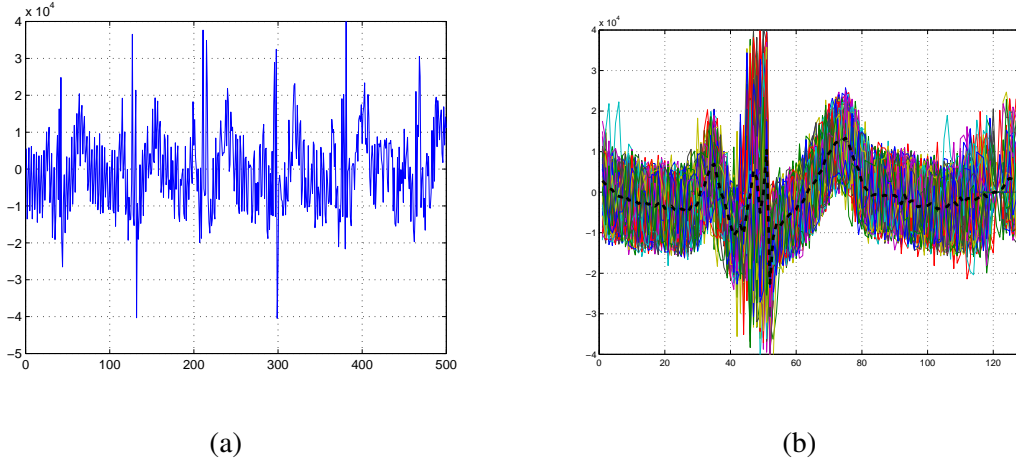


Fig. 8. Effect of the powerline interference phenomenon over the proposed curve alignment method: distorted signal (a), and aligned pulses with the average ECG pulse obtained for one block (b)

As shown in the latter Figure, the proposed algorithm is robust for this kind of distortion, as we retrieve about the same average signal after alignment of the curves. It shall be noted, once again, that this kind of perturbation can interfere with the segmentation procedure, and that for interferences with high amplitude, a prefiltering step as described in [20], [21], [22] could be applied. Both results illustrate the robustness of semiparametric methods for curve alignment, when compared to standard FDA analysis. We now apply the proposed algorithm to a real ECG signal displayed in Figure 9, which is distorted by powerline interference and baseline wander. After a preliminary segmentation, we get the individual pulses displayed in Figure 10. The aligned curves and the obtained average signal are presented in Figure 11. It can be noted that the proposed method still performs well and is robust to aforementioned perturbations. The obtained average signal is therefore more representative.

D. Discussion

Figures 3(b) and 3(c) are a good illustration of Proposition 3.2. Figure 3(c) shows that when λ is too small, the curves are well aligned within the blocks, but blocks have different constant shift. Taking a larger λ addresses this problem, as it can be seen in Figure 3(b). Our proposed method uses all the available information and not only the information contained in the neighborhood of the landmarks. The advantage of our method is evident with noisy curves, when locating the maximum of each curve is very difficult.

Not surprisingly, the number of curves in each block K may be low if the noise variance remains very small (first column of Table I), the limiting case $K = 2$ consisting in aligning the curves individually. Theoretically, K should be taken as large as possible. However, this comes with a price, the larger the K the more difficult is the optimization problem.

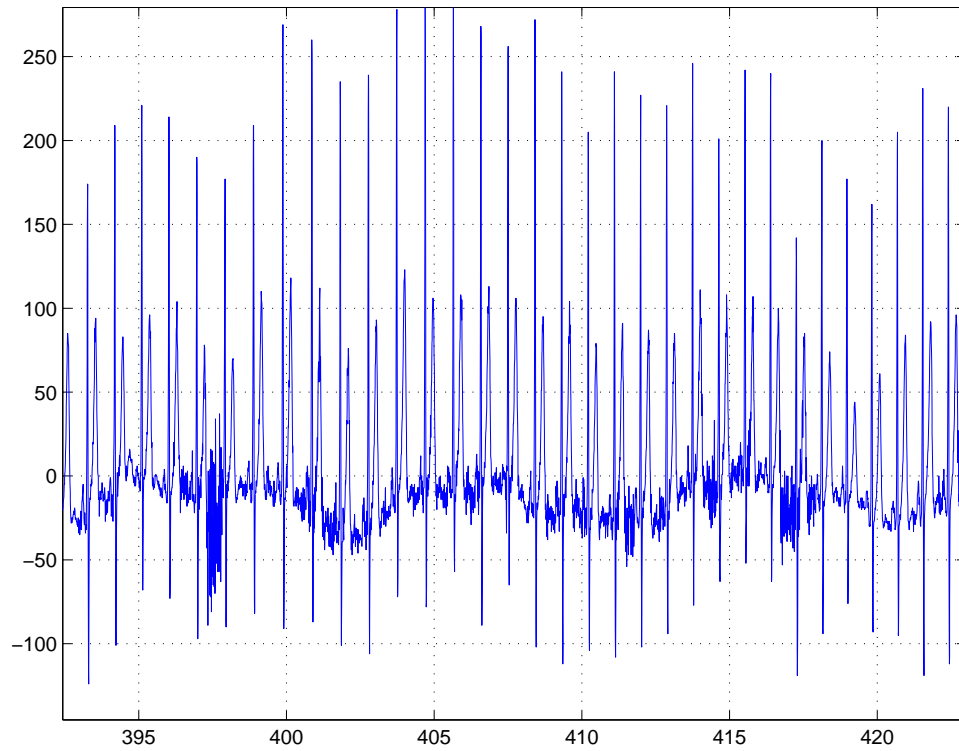


Fig. 9. ECG signal with real baseline wander and powerline interference (partial)

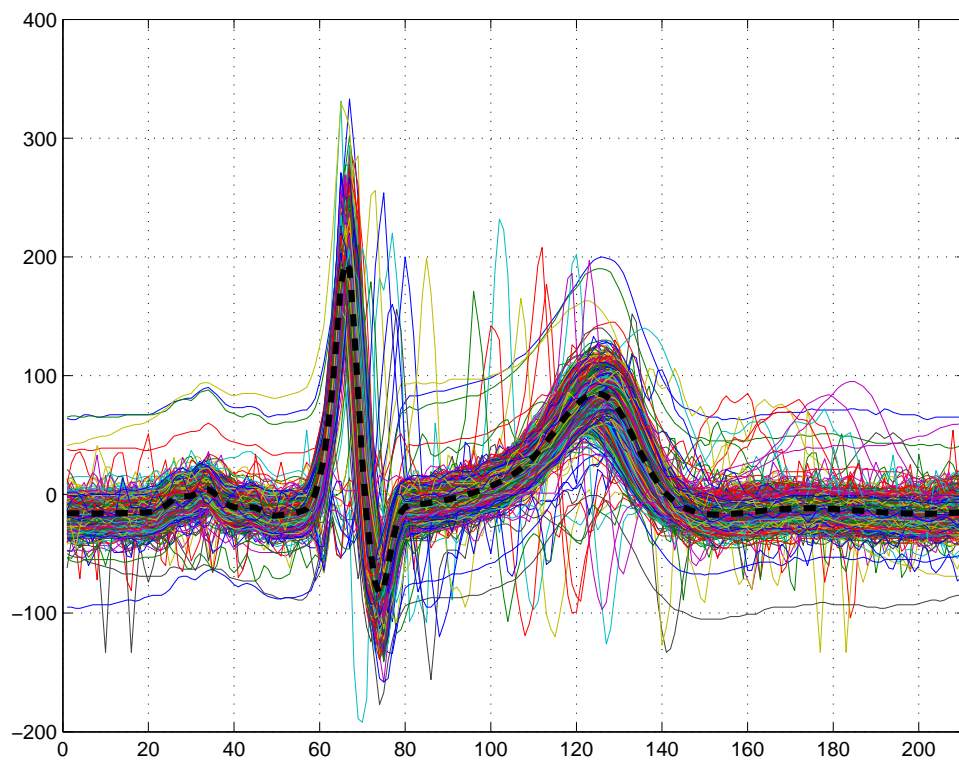


Fig. 10. Obtained curves before the curve alignment procedure and associated average signal (dotted).

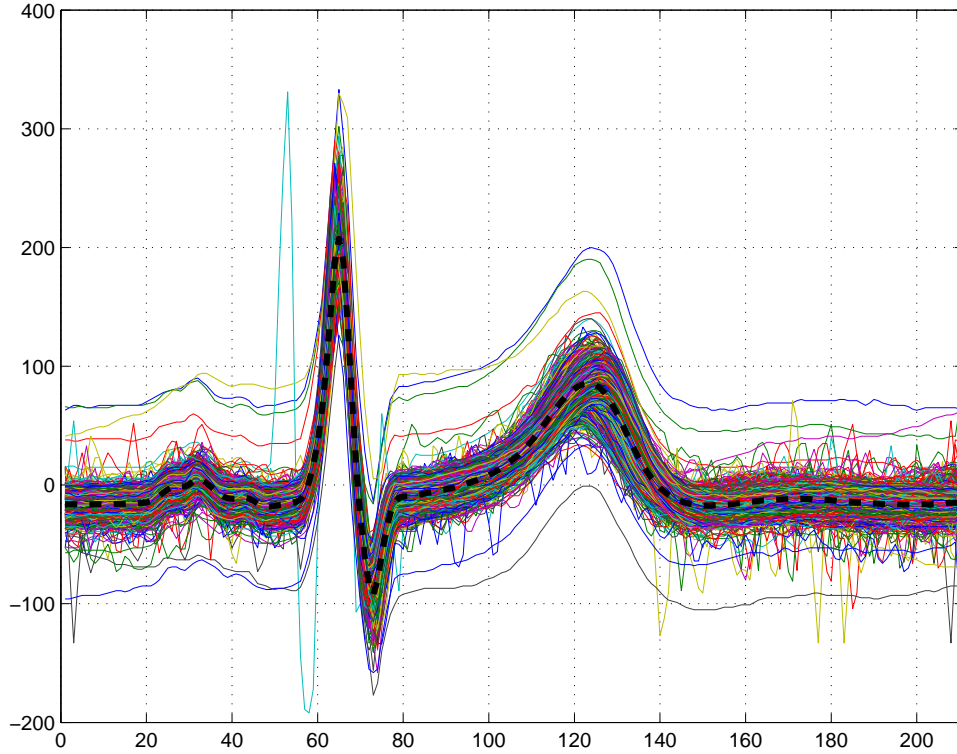


Fig. 11. Aligned curve by means of the proposed method, and average curve (dotted).

M-estimation for curve alignment is also discussed in [11]. In fact, [11, Theorem 2.1] shows that a statistically consistent alignment can be obtained only when filtering the curves and aligning the low-frequency information. Therefore, an approach based on the spectral information is more likely to achieve good alignment by comparison to the standard method of [1]. Still, the choice of the parameter K of our method is easier than the choice of the sequence $\{\delta_j, j \in \mathbb{Z}\}$ needed for the estimator described in [11].

V. CONCLUSION

We proposed in this paper a method for curve alignment and density estimation of the shifts, based on an M-estimation procedure on a functional of the power spectrum density. The proposed estimator, deduced from blocks of curves of size K , showed good performances in simulations, even when the noise variance is high. On real ECG data, the proposed method outperforms the functional data analysis method, thus leading to a more meaningful average signal, which is of interest for the study of some cardiac arrhythmias. Investigations of the associated kernel estimates, with emphasis on rates of convergence, should appear in a future contribution.

VI. ACKNOWLEDGMENTS

We are grateful to the French International Volunteer Exchange Program, who partially funded the present work. We would like to thank Y. Isserles for helping comments while writing the paper.

APPENDIX

A. Computation of the noise-free part

If the curves are perfectly aligned, that is if $\alpha_1 = \theta_1$, equation (10) becomes

$$\begin{aligned}
B_1(k, \theta_1) &= \frac{|c_s(k)|^2}{(\lambda + K)^2} \sum_{l,m=0}^K \lambda_l \lambda_m \\
&+ \frac{\sigma^2}{n(\lambda + K)^2} \sum_{l,m=0}^K \lambda_l \lambda_m \{e^{ik(\theta_l - \theta_m)} \times \\
&[V_{k,l}V_{k,m} + W_{k,l}W_{k,m} + i(V_{k,l}W_{k,m} - W_{k,l}V_{k,m})]\} \\
&+ \frac{\sigma c_s(k)}{\sqrt{n}(\lambda + K)^2} \sum_{l,m=0}^K \lambda_l \lambda_m e^{-i\theta_m} (V_{k,m} - iW_{k,m}) \\
&+ \frac{\sigma c_s^*(k)}{\sqrt{n}(\lambda + K)^2} \sum_{l,m=0}^K \lambda_l \lambda_m e^{ik\theta_l} (V_{k,l} + iW_{k,l})
\end{aligned} \tag{15}$$

Equation (10) can also be expanded, in order to find a equation close to (9). We find after some calculations that

$$\begin{aligned}
B_1(k, \theta_1) &= |c_s(k)|^2 + \frac{\sigma^2}{n(\lambda + K)^2} \sum_{l=0}^K \lambda_l^2 (V_{k,l}^2 + W_{k,l}^2) \\
&+ \frac{2\lambda\sigma^2}{n(\lambda + K)^2} \text{Re}\left\{\sum_{l=1}^K e^{ik\theta_l} [V_{k,l}V_{k,0} + W_{k,l}W_{k,0} \right. \\
&\quad \left. + i(V_{k,l}W_{k,0} - W_{k,l}V_{k,0})]\right\} \\
&+ \frac{2\sigma^2}{n(\lambda + K)^2} \text{Re}\left\{\sum_{1 \leq l < m \leq K} e^{ik\theta_l} [V_{k,l}V_{k,m} + W_{k,l}W_{k,m} \right. \\
&\quad \left. + i(V_{k,l}W_{k,m} - W_{k,l}V_{k,m})]\right\} \\
&+ \frac{2\sigma \text{Re}(c_s(k))}{\sqrt{n}(\lambda + K)} \sum_{l=0}^K \lambda_l (V_{k,l} \cos(k\theta_l) - W_{k,l} \sin(k\theta_l)) \\
&- \frac{2\sigma \text{Im}(c_s(k))}{\sqrt{n}(\lambda + K)} \sum_{l=0}^K \lambda_l (V_{k,l} \sin(k\theta_l) + W_{k,l} \cos(k\theta_l))
\end{aligned} \tag{16}$$

Collecting equations (9), (10) and (16), we can check easily that the only noise-free part comes from the second sum in (8), and is equal to $D_1(\alpha_1)$.

B. Proof of Proposition 3.1

Using Equations (9) and (16), we get that for all k the deterministic part of $A_M(k) - B_1(k, \boldsymbol{\theta}_1)$ vanishes, leading to

$$\begin{aligned}
A_M(k) - B_1(k, \boldsymbol{\theta}_1) &= \frac{\sigma^2}{(M+1)n} \sum_{l=0}^M (V_{k,l}^2 + W_{k,l}^2) \\
&- \frac{\sigma^2}{n(\lambda + K)^2} \sum_{l=0}^K \lambda_l^2 (V_{k,l}^2 + W_{k,l}^2) \\
&- \frac{2\lambda\sigma^2}{n(\lambda + K)^2} \operatorname{Re}\left\{ \sum_{l=1}^K e^{ik\theta_l} [V_{k,l}V_{k,0} + W_{k,l}W_{k,0} \right. \\
&\quad \left. + i(V_{k,l}W_{k,0} - W_{k,l}V_{k,0})] \right\} \\
&- \frac{2\sigma^2}{n(\lambda + K)^2} \operatorname{Re}\left\{ \sum_{1 \leq l < m \leq K} e^{ik\theta_l} [V_{k,l}V_{k,m} + W_{k,l}W_{k,m} \right. \\
&\quad \left. + i(V_{k,l}W_{k,m} - W_{k,l}V_{k,m})] \right\} \\
&+ \frac{2\sigma \operatorname{Re}(c_s(k))}{(M+1)\sqrt{n}} \sum_{l=0}^M (V_{k,l} \cos(k\theta_l) - W_{k,l} \sin(k\theta_l)) \\
&- \frac{2\sigma \operatorname{Im}(c_s(k))}{(M+1)\sqrt{n}} \sum_{l=0}^M (V_{k,l} \sin(k\theta_l) + W_{k,l} \cos(k\theta_l)) \\
&- \frac{2\sigma \operatorname{Re}(c_s(k))}{\sqrt{n}(\lambda + K)} \sum_{l=0}^K \lambda_l (V_{k,l} \cos(k\theta_l) - W_{k,l} \sin(k\theta_l)) \\
&+ \frac{2\sigma \operatorname{Im}(c_s(k))}{\sqrt{n}(\lambda + K)} \sum_{l=0}^K \lambda_l (V_{k,l} \sin(k\theta_l) + W_{k,l} \cos(k\theta_l)).
\end{aligned}$$

All the above sums are of i.i.d. random variables, with mean zero (except for the first two sums), and all have sub-Gaussian tails. Consequently, there is a constant D , independent of k , such that when $K \rightarrow \infty$, $\lambda \rightarrow \infty$ and $\lambda/K \rightarrow 0$:

$$\|A_M(k) - B_1(k, \boldsymbol{\theta}_1)\|_{\mu_2} \leq D \left(\frac{\sigma^2}{nK} + \frac{\sigma|c_s(k)|}{\sqrt{nK}} \right)$$

where for any random variable X , $\|X\|_{\mu_2} = \sqrt{\mathbb{E}(X^2)}$. Hereafter, D is the same constant, large enough to keep all the inequalities valid. From the latter inequality, we get that:

$$\sum_{k \in \mathcal{K}} \nu_k (A_m(k) - B_1(k, \boldsymbol{\theta}_1))^2 = O_{\mathbb{P}}\left(\frac{1}{n^2}\right) + O_{\mathbb{P}}\left(\frac{1}{nK}\right).$$

We now study the term $R(k)$, that is the part of $B_1(k, \boldsymbol{\theta}_1) - B_1(k, \boldsymbol{\alpha}_1)$ which depends on the random variables V and W , using their expression in (10) and (15). We get that $R(k) = I + II + III$, where

$$I \triangleq \frac{\sigma^2}{n(\lambda + K)^2} \left| \sum_{l=0}^K \lambda_l e^{ik\alpha_l} (V_{k,l} + iW_{k,l}) \right|^2$$

$$II \triangleq -\frac{\sigma^2}{n(\lambda + K)^2} \left| \sum_{l=0}^K \lambda_l e^{ik\theta_l} (V_{k,l} + iW_{k,l}) \right|^2$$

and

$$III \triangleq 2\text{Re}\left\{ \frac{c_s(k)\sigma}{\sqrt{n}(\lambda + K)^2} \sum_{l,m=0}^K \lambda_l \lambda_m \times \right. \\ \left. (e^{ik(\alpha_l - \theta_l - \alpha_m)} - e^{-ik\theta_m})(V_{k,m} - iW_{k,m}) \right\}$$

Write $I = I_1 + I_2 + I_3 + I_4$, where

$$I_1 \triangleq \frac{\sigma^2}{n(\lambda + K)^2} \lambda^2 (V_{k,0}^2 + W_{k,0}^2) \\ I_2 \triangleq \frac{2\lambda\sigma^2}{n(\lambda + K)^2} \sum_{l=1}^K \cos(k\alpha_l) (V_{k,l}V_{k,0} + W_{k,l}W_{k,0}) \\ I_3 \triangleq \frac{2\sigma^2}{n(\lambda + K)^2} \sum_{1 \leq l < k \leq K} [\cos(k(\alpha_l - \alpha_m)) (V_{k,l}V_{k,m} \\ + W_{k,l}W_{k,m})] \\ I_4 \triangleq \frac{\sigma^2}{n(\lambda + K)^2} \sum_{l=1}^K (V_{k,l}^2 + W_{k,l}^2)$$

It is obvious that $\|I_1\|_{\mu_2} \leq \frac{D\sigma^2}{nK}$, as $K \rightarrow \infty$ and $\lambda/K \rightarrow 0$. Moreover, the sum in the term I_4 has a chi-square distribution with $2K$ degrees of freedom, and is the of same order as I_1 . Finally, observe that I_2 and I_3 are sums of terms with zero mean and bounded variance. Since

$$|I_3| \leq \frac{2\sigma^2}{n(\lambda + K)^2} \sum_{1 < l < k \leq K} |V_{k,l}V_{k,m} + W_{k,l}W_{k,m}|,$$

we get that $\|I_3\|_{\mu_2} \leq D\sigma^2/n$, I_2 being bounded similarly. We obtain that $\|I_2 + I_3\|_{\mu_2} \leq D\sigma^2/n$. Thus, $\|I\|_{\mu_2} \leq D\sigma^2/n$. II is a sum of independent random variables with zero mean and bounded variance, hence $\|II\|_{\mu_2} \leq D\sigma^2/nK$. Finally, observe that $III = A - B$, where

$$A \triangleq 2\text{Re}\left\{ \frac{c_s(k)\sigma}{\sqrt{n}(\lambda + K)^2} \right. \\ \left. \times \sum_{l=0}^K \lambda_l e^{ik(\alpha_l - \theta_m)} \times \sum_{m=0}^K \lambda_m e^{-ik\alpha_m} (V_{k,m} - iW_{k,m}) \right\}$$

and

$$B \triangleq 2\text{Re}\left\{ \frac{c_s(k)\sigma}{\sqrt{n}(\lambda + K)^2} \right. \\ \left. \cdot \sum_{l=0}^K \lambda_l \times \sum_{m=0}^K \lambda_m e^{-ik\theta_m} (V_{k,m} - iW_{k,m}) \right\}$$

The first sums in A and B are bounded by $K + \lambda$ and the second sums are of K independent random variables with expectation equal to 0 and bounded variances, hence $\|A - B\|_{\mu_2} \leq D(\sigma|c_s(k)|/\sqrt{nK})$.

Recall that $\sum_{\nu \in \mathcal{K}} \nu_k$ is bounded. Equation (12) is obtained if all the bounds above are collected, and Assumption (H-2) is used. Eventually, we can check easily that $\|B_1(k, \alpha_1) - B_1(k, \theta_1)\|_{\mu_2} < \infty$, and obtain the last equality of (12) by means of Hölder's inequality.

C. Proof of Proposition 3.2

Observe that there exists γ_0 in $(0, 1)$ such that, for all x in $[-\pi, \pi]$, we have $\cos x \leq 1 - \gamma_0 x^2$. Since we have

$$\left| \frac{1}{(K + \lambda)} \sum_{0 \leq m \leq K} \lambda_l \exp(ik(\theta_m - \alpha_m)) \right| \leq 1 ,$$

then there exists, according to the assumption, two constants $K_0 \geq 0$ and c such that, for $K \geq K_0$ and every k , we have

$$\operatorname{Re} \left(\frac{e^{-ic}}{(K + \lambda)} \sum_{0 \leq m \leq K} \lambda_l \exp(ik(\theta_m - \alpha_m)) \right) \geq 1 - \eta , \quad (17)$$

where $\operatorname{Re}(z)$ denotes the real part of the complex number z . Hence

$$\begin{aligned} 1 - \eta &\leq \frac{1}{K + \lambda} \sum_{m=1}^K \cos(k(\theta_m - \alpha_m - c)) \\ &\leq \frac{1}{K + \lambda} \sum_{m=1}^K (1 - \gamma_0 k^2 (\theta_m - \alpha_m - c)^2), \end{aligned}$$

and (13) follows. Denote by N the number of curves in the block whose alignment error is “far” from c (up to a 2π factor):

$$N \triangleq \sum_{m=1}^K \mathbf{1} \left\{ |\theta_m - \alpha_m - c| \geq \eta^\delta \right\} ,$$

and assume, for simplicity, that the N last curves are the misaligned curves. Equation (17) implies

$$\begin{aligned} 1 - \eta &\leq \frac{1}{K + \lambda} \sum_{m=0}^{K-N-1} \cos(k(\theta_m - \alpha_m - c)) \\ &\quad + \frac{1}{K + \lambda} \sum_{m=N-K}^K \cos(k(\theta_m - \alpha_m - c)) \\ &\leq \frac{K + \lambda - N}{K + \lambda} + \frac{N}{K} (1 - \gamma_0 k^{2\delta} \eta^{2\delta}) \\ &= 1 - \frac{N}{K + \lambda} \gamma_0 k^{2\delta} \eta^{2\delta} . \end{aligned} \quad (18)$$

Equation (18) leads to

$$N \leq \frac{K + \lambda}{\gamma_0 k^{2\delta}} \eta^{1-2\delta} ,$$

which completes the proof.

D. Proof of Proposition 3.3

Assume that $|c| > \eta^\delta$; since λ is assumed to be an integer, we can see this weighting parameter as the artificial addition of $\lambda - 1$ reference curves. Since $\alpha_0 = \theta_0 \triangleq 0$, in that case, $|\theta_0 - \alpha_0 - c| > \eta^\delta$, thus giving

$$\frac{N}{K + \lambda} > \frac{\lambda}{K + \lambda} \geq \gamma \eta^{1-2\delta},$$

which would contradict Proposition 3.2. Therefore, we get that $|c| \leq \eta^\delta$.

REFERENCES

- [1] B. W. Silveanu and J. Ramsay, *Functional Data Analysis*, 2nd ed. Springer Series in Statistics, 2005.
- [2] F. Ferraty and P. Vieu, *Nonparametric Functional Data Analysis: Theory and Practice*, 1st ed. Springer Series in Statistics, 2006.
- [3] J. O. Ramsay, “Estimating Smooth Monotone Functions,” *Journal of the Royal Statistical Society Series B*, vol. 60, no. 2, pp. 365–375, 1998.
- [4] J. O. Ramsay and X. Li, “Curve Registration,” *Journal of the Royal Statistical Society Series B*, vol. 60, no. 2, pp. 351–363, 1998.
- [5] B. Ronn, “Nonparametric Maximum Likelihood Estimation for Shifted Curves,” *Journal of the Royal Statistical Society Series B*, vol. 63, no. 2, pp. 243–259, 2001.
- [6] T. Gasser and A. Kneip, “Searching for Structure in Curve Sample,” *Journal of the American Statistical Association*, vol. 90, no. 432, pp. 1179–1188, 1995.
- [7] A. Kneip and T. Gasser, “Statistical Tools to Analyze Data Representing a Sample of Curves,” *Annals of Statistics*, vol. 20, no. 3, pp. 1266–1305, 1992.
- [8] A. C. Guyton and J. E. Hall, *Textbook of Medical Physiology*, 9th ed. W. H. Saunders, 1996.
- [9] J. Pan and W. Tomkins, “A Real Time QRS Detection Algorithm,” *IEEE Transactions on Biomedical Engineering*, vol. 32, no. 3, pp. 230–236, 1985.
- [10] D. Chafaï and J.-M. Loubes, “Maximum Likelihood for a Certain Class of Inverse Problems: an Application to Pharmacokinetics,” *Statistics and Probability Letters*, vol. 76, pp. 1225–1237, 2006.
- [11] F. Gamboa, J.-M. Loubes, and E. Maza, “Semiparametric Estimation of Shifts Between Curves,” *Electronic Journal of Statistics*, vol. 1, pp. 616–640, 2007.
- [12] M. Lavielle and C. Levy-Leduc, “Semiparametric Estimation of the Frequency of Unknown Periodic Functions and its Application to Laser Vibrometry Signals,” *IEEE Transactions in Signal Processing*, vol. 53, no. 7, pp. 2306–2314, 2005.
- [13] Y. Ritov, “Estimating a Signal with Noisy Nuisance Parameters,” *Biometrika*, vol. 76, no. 1, pp. 31–37, 1989.
- [14] I. Castillo, “Estimation Semi-Paramétrique à l’Ordre 2 et Applications,” Ph.D. dissertation, Université Paris XI, 2006.
- [15] T. Trigano, U. Isserles, and Y. Ritov, “Semiparametric Shift Estimation for Alignment of ECG Data,” in *Proceedings of the EUSIPCO Signal Processing Conference*, 2008.
- [16] O. Sayadi and M. B. Shamsollahi, “Multiadaptive Bionic Wavelet Transform: Application to ECG Denoising and Baseline Wandering Reduction,” *EURASIP Journal on Advances in Signal Processing*, vol. 2007, pp. 1–11, 2007.
- [17] M. A. Mneimneh, E. E. Yaz, M. T. Johnson, and R. J. Povinelli, “An Adaptive Kalman Filter for Removing Baseline Wandering in ECG Signals,” *Computers in Cardiology*, vol. 33, pp. 253–256, 2006.
- [18] B. Mozaffary and M. A. Tinati, “ECG Baseline Wander Elimination using Wavelet Packets,” in *Proceedings of World Academy of Science, Engineering and Technology*, vol. 3, 2005.

- [19] L. D. Avendano-Valencia, L. E. Avendano, J. M. Ferrero, and G. Castellanos-Dominguez, "Improvement of an Extended Kalman Filter Power Line Interference Suppressor for ECG Signals," *Computers in Cardiology*, vol. 34, pp. 553–556, 2007.
- [20] I. Christov, "Dynamic Powerline Interference Subtraction from Biosignals," *Journal of Medical Engineering and Technology*, vol. 24, no. 4, pp. 169–172, 2000.
- [21] C. Levkov, G. Mihov, R. Ivanov, I. Daskalov, I. Christov, and I. Dotsinsky, "Removal of Power-Line Interference from the ECG: a Review of the Subtraction Procedure," *BioMedical Engineering OnLine*, vol. 4, no. 50, pp. 1–18, 2005.
- [22] A. K. Ziarani and A. Konrad, "A Nonlinear Adaptive Method of Elimination of Power Line Interference in ECG Signals," *IEEE Transactions on Biomedical Engineering*, vol. 49, no. 6, pp. 540–547, 2002.